Effect of process parameters on the structure of Si–Ti–N nanostructured coatings deposited by hypersonic plasma particle deposition

J. Hafiz [a,*], R. Mukherjee [a], X. Wang [a], M. Marshall [b], R.D. Twesten [b], M. Cullinan [c], J.V.R. Heberlein [a], P.H. McMurry [a], S.L. Girshick [a]

[a] Department of Mechanical Engineering, University of Minnesota, 111 Church St. SE, Minneapolis, MN 55455, USA
[b] Center for Microanalysis of Materials, University of Illinois at Urbana-Champaign, 104 South Goodwin Avenue, Urbana, IL 61801, USA
[c] Department of Engineering, Swarthmore College, 500 College Avenue, Swarthmore, PA 19081, USA

Available online 17 October 2005

Abstract

Si–Ti–N nanostructured coatings were synthesized by inertial impaction of nanoparticles using a process called hypersonic plasma particle deposition (HPPD). A study detailing the effect of plasma gases showed that in the case of an $Ar+H_2$ plasma gas mixture, crystalline phases in the coatings consisted of TiN, $TiSi_2$, and Ti_5Si_3. When the system was switched to a plasma gas mixture of $Ar+N_2$, the only crystalline phase was TiN. Transmission electron microscopy confirmed the presence of TiN crystallites in an amorphous matrix. Warren–Averbach analysis indicated the average size of the TiN crystallites to be 14.9 nm. In separate experiments with the same conditions, aerodynamic lenses were used to deposit particles directly onto TEM grids. We observed agglomerated structures with an $Ar+N_2$ plasma, while with an $Ar+H_2$ plasma we found discrete $TiSi_x$ and TiN_x particles. In-situ particle diagnostics indicated only small changes in the particle size distributions when the plasma gases were changed.
© 2005 Published by Elsevier B.V.

Keywords: Inertial impaction; Nanostructure; Aerodynamic lens; Hypersonic

1. Introduction

Nanocomposite Si–Ti–N coatings have generated considerable attention as various researchers have highlighted their improved mechanical properties, enhanced thermal stability, and oxidation resistance. A variety of film deposition methods have been employed to synthesize Si–Ti–N coatings, such as hybrid arc sputtering [1], reactive magnetron sputtering [2], chemical vapor deposition [3,4], and ion plating [5]. The structure and properties of these coatings depend directly on the process parameters and deposition conditions. Consequently, a good understanding of the effect of different process conditions is needed to enhance the mechanical properties of Si–Ti–N coatings.

We have previously reported on Si–Ti–N nanostructured coatings synthesized by inertial impaction of nanoparticles using a process called hypersonic plasma particle deposition (HPPD) [6]. In this paper, we present results concerning the effect of HPPD process conditions on the properties of Si–Ti–N coatings. The effect of plasma gas composition ($Ar+H_2$ or $Ar+N_2$) on the morphology and structure of the coatings is reported. We also analyzed the size, composition and morphology of individual particles synthesized under the same conditions and collected downstream on transmission electron microscope (TEM) grids utilizing an aerodynamic lens assembly [7,8]. Typical grain sizes of samples deposited using the lens assembly were compared with in-situ size distributions measured by our nanoparticle diagnostic system [9]. Particle diagnostics provide insight into the mechanism of particle formation and growth, and may enable optimization of operating conditions to achieve desired film properties.

* Corresponding author.
   E-mail address: jhafiz@me.umn.edu (J. Hafiz).

2. Experimental details

2.1. Deposition process

HPPD utilizes a DC arc discharge to synthesize particles and is a one-step process that occurs in a controlled environment. Details of the HPPD setup have been presented previously [6,10]. For Si–Ti–N deposition, SiCl$_4$ (20 sccm), TiCl$_4$ (140 sccm) and NH$_3$ (500 sccm) vapors were injected into the plasma where the temperatures are sufficiently high ($\sim$ 4000 °C) to dissociate the vapor phase reactants. Particle synthesis is achieved by quenching the hot gas in a rapid nozzle expansion. Particles are deposited on a molybdenum substrate by hypersonic impaction to form Si–Ti–N coatings. The coatings were $\sim$ 50 μm thick for a deposition time of 3 min. Typical substrate temperature during deposition ranged from 750 to 850 °C.

In order to collect particles on TEM grids for off-line analysis, the molybdenum substrate was removed and replaced with an aerodynamic lens assembly [7], located approximately 1 m downstream of the nozzle. A brief description of the aerodynamic lens assembly is given here. The lens system consists of a set of five thin-plate orifices (lenses) mounted inside a barrel. The gas inside the lens assembly contracts and expands as it passes through each of the lenses. Sufficiently small particles follow the gas, whereas large particles are lost to the walls. Particles of intermediate sizes are pushed closer toward the centerline. Our lens assembly focuses 10–100 nm particles into a collimated beam with a diameter of a few tens of microns. A critical orifice is placed at the end of the barrel, beyond which the flow undergoes another expansion. The nanoparticle beam then deposits at room temperature on a translatable substrate containing TEM grids for off-line analysis.

2.2. Characterization techniques

In-situ particle size distribution measurements were performed using a sampling probe interfaced to an extraction/dilution system in series with a scanning electrical mobility spectrometer (SEMS). The SEMS system converts particles of different shapes and sizes into equivalent mobility diameters. Details of the sampling system are presented elsewhere [9]. During measurements, the Mo substrate was removed and replaced with the sampling probe. The probe was placed 20 mm away from the nozzle, corresponding to the substrate standoff distance for film deposition (Fig. 1).

The hypersonically deposited coatings were investigated using various characterization tools. X-ray diffraction (XRD) spectra were obtained with a Bruker AXS microdiffractometer (CuKα). X-ray photoelectron spectroscopy (XPS) was carried out with a PHI-5400 model equipped with an Al X-ray source. For analytical transmission electron microscopy we used a VG HB501 STEM (Scanning Transmission Electron Microscope), equipped with an energy dispersive spectrometer (EDS), as well as a Gatan DigiPEELS parallel electron energy loss spectrometer (PEELS). EDS analysis is not particularly sensitive to light elements such as nitrogen. This obstacle was overcome by PEELS analysis, which allowed for the detection of nitrogen.

For high resolution imaging we used a conventional JEOL 2010 FEG TEM. Samples from the coatings were prepared for TEM analysis using the focused ion beam (FIB) milling technique [11]. Using a FEI Strata DB235 FIB, electron transparent cross sections of the coatings were prepared. Samples collected through the lens assembly did not require similar preparation, as they were deposited directly onto TEM grids.

3. Results and discussion

3.1. Effect of plasma gas composition

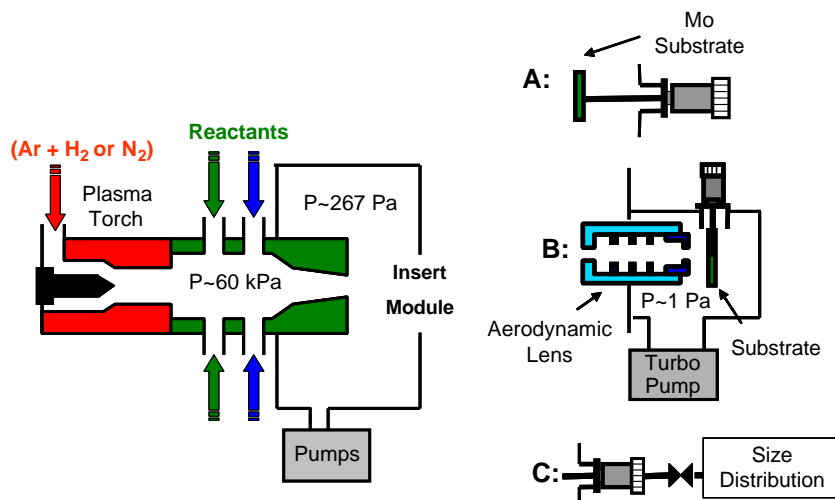To determine the effect of plasma gases on coating properties, we synthesized coatings with a plasma gas

Fig. 1. Schematic of the HPPD system.

mixture of either Ar+N$_2$ (30 slm+2.5 slm) or Ar+H$_2$ (30 slm+2.5 slm). For both cases the reactant flow rates were identical. X-ray diffraction spectra of films synthesized with a plasma gas mixture of Ar+H$_2$ show the presence of crystalline TiN, TiSi$_2$, and Ti$_5$Si$_3$, while films synthesized with an Ar+N$_2$ mixture show only crystalline TiN (Fig. 2). The difference in crystalline phases present in the coatings can be attributed to the effect of extra nitrogen available during the synthesis process. Studies on the phase stability of Si−Ti−N have indicated that nitrogen activity plays a key role in changing phase components [12]. When the partial pressure of N is sufficiently high, Si does not form a stable titanium silicide phase. In addition, availability of excess N$_2$ also favorably affects the kinetics of film formation process during Si−Ti−N deposition [3]. In our system, the partial pressure of nitrogen is increased significantly by adding extra N$_2$ as one of the plasma gases, resulting in the formation of only TiN with Si existing in an amorphous phase. These results indicate that we can switch crystalline phases in our coatings by changing our plasma gases.

3.2. Crystallite size and composition measurements

For transmission electron microscopy we prepared a sample synthesized with an Ar+N$_2$ mixture by FIB milling. The TEM image highlights lattice fringes of nanocrystallites embedded in an amorphous matrix, while the corresponding EDS spectra show the presence of Si and Ti (Fig. 3). Nitrogen is absent from the spectra due to EDS limitations, as mentioned earlier. To determine the composition of the crystallites, we took higher resolution images and calculated an average lattice fringe spacing (Fig. 4). The fringe spacing was measured to be 0.2119 nm, closely corresponding to the (200) phase of TiN, which has a lattice spacing of 0.212 nm. XPS results indicate that the amorphous matrix consists of Si$_3$N$_4$.
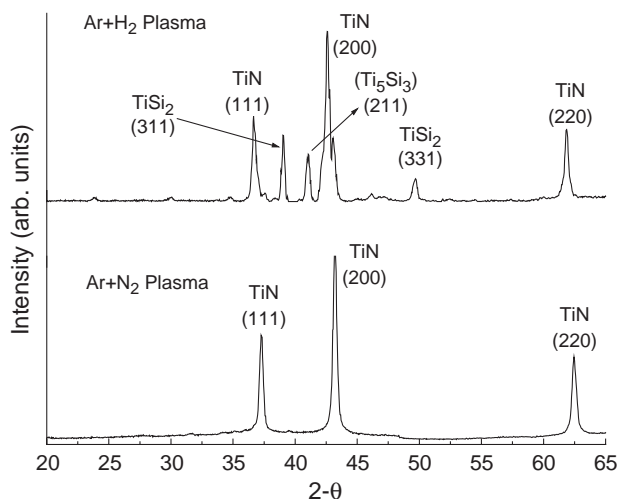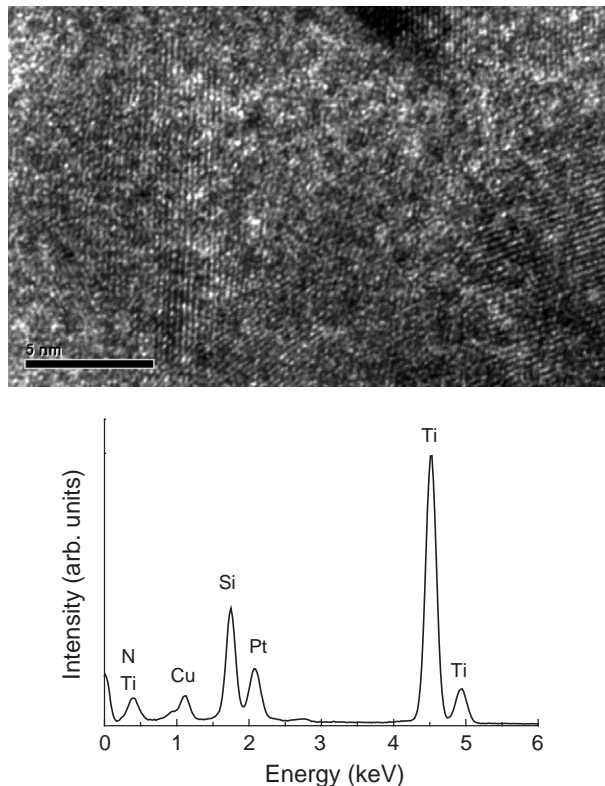

Fig. 3. TEM image of a Focused Ion Beam (FIB) milled sample and corresponding EDS spectra. The Pt appears from a conductive coating while Cu comes from the TEM grid.

It is difficult to accurately calculate the sizes of nanocrystals present in the sample due to gallium ion induced damage as a result of FIB milling. Average crystallite size determined from the broadening of Bragg reflections using the Warren−Averbach method [13] show the average size of TiN crystals to be 14.9 nm. If on average the nanocrystals are larger than 10 nm, it would provide a reason for the maximum hardness values (~28 GPa) we have achieved so far. The construction of superhard nanocomposite coatings is based on the synthesis of TiN nanocrystallites in the range of 3−10 nm
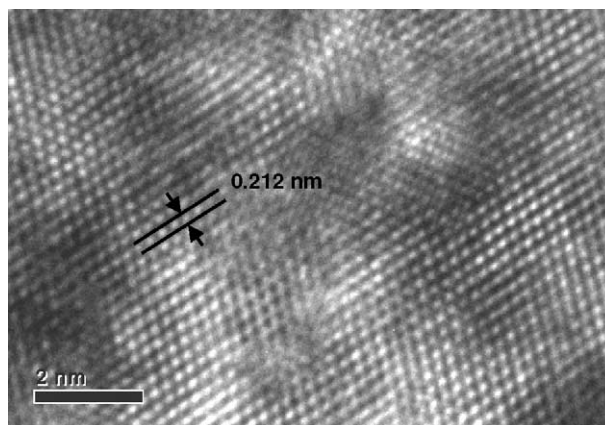

Fig. 2. X-ray diffraction spectra of Si−Ti−N coatings deposited with an Ar+H$_2$ plasma gas mixture (top) and an Ar+N$_2$ mixture (bottom).

Fig. 4. High-resolution TEM image of an embedded crystallite.

surrounded by an amorphous matrix of Si_3N_4. Additionally, the ideal separation between the TiN nanocrystals should be about one monolayer of Si_3N_4 to attain high hardness [14]. At these conditions both dislocations and incoherent stress relaxation are hindered, resulting in superhardness. Our coatings show large crystallite sizes (>10 nm), sufficient for the formation and propagation of dislocations. This restricts the hardness that we can achieve with our coatings.

3.3. Grain structure of nanoparticles collected after aerodynamic lenses

An aspect of the HPPD process that provided us with some understanding of the particle formation process was the effect of residence time and temperature history. By removing the Mo substrate and allowing the particles to cool to room temperature, we could analyze how process parameters affect particle growth and morphology. Samples were collected for these experiments by removing the Mo substrate and passing particles through an aerodynamic lens assembly located approximately 1 m downstream of the nozzle. While it is interesting to analyze particles sampled this way, it is important to note that due to the
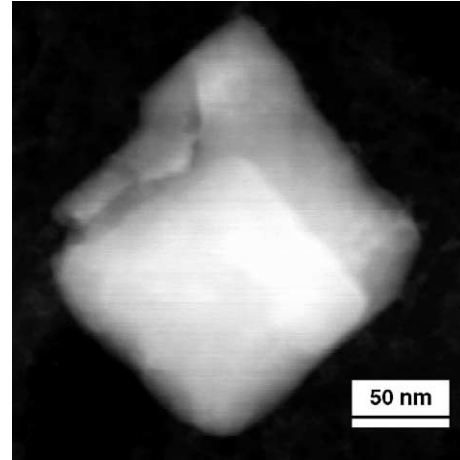

Fig. 6. TEM image of a cube-like particle prepared using an Ar+H_2 plasma.

difference in residence time and temperature history, the samples may not be representative of the coatings formed by ballistic impaction.

Particles synthesized using an Ar+H_2 plasma and collected on TEM grids were primarily spherical in nature and non-agglomerated. There were also some cube-like structures present. The majority of the particles were 30 nm or greater in diameter. The relatively large size is due to the longer residence time, which allows sufficient time for growth to occur in comparison to particles that impact the substrate to form our coatings. Additionally, there are not many small particles (<10 nm) as the aerodynamic lenses do not effectively focus smaller particles. An EDS linescan of a spherical particle shows the presence of Ti, Si and O. Oxygen is expected to form an oxide layer, as $TiSi_2$ may form an SiO_2 layer due to Si diffusion to the surface (Fig. 5) [15]. Analysis shows that for these particles oxygen is diffused throughout (atomic concentration as high as 20%). Fig. 6 highlights a cube-like particle observed in the sample. PEELS spectra of the spherical
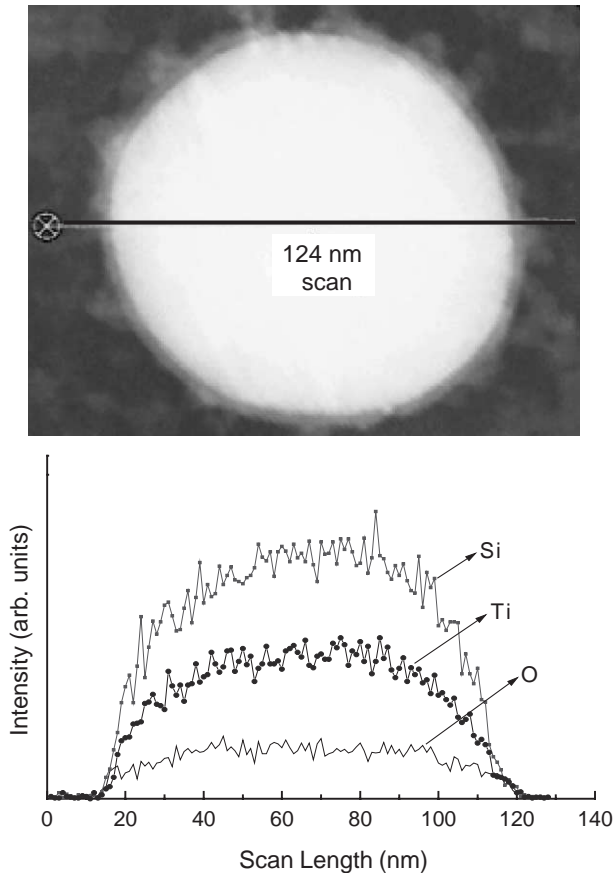

Fig. 5. EDS linescan of a spherical particle synthesized using an Ar+H_2 plasma and collected on a TEM grid utilizing the aerodynamic lenses. The scan was taken along the line shown on the TEM image.
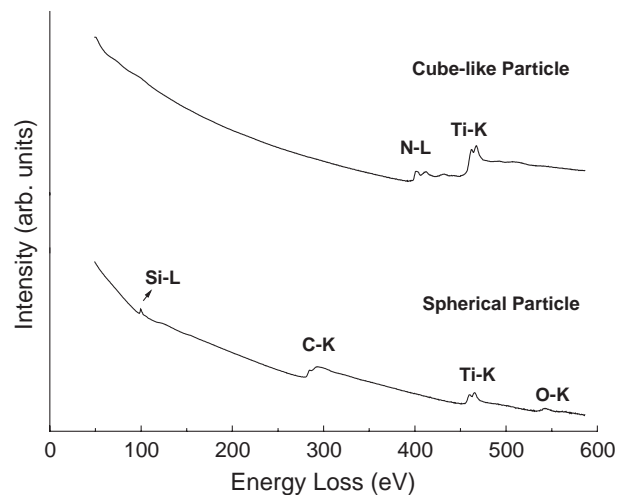

Fig. 7. PEELS spectra of a cube-like particle (top) and a spherical particle (bottom).

particle confirm the presence of Ti, Si, and O but indicate a lack of nitrogen in the sample, while analysis of the cube-like particle shows the presence of Ti and N indicating that the structure is TiN_x (Fig. 7). Compared to the Ti and the N peak, the Si peak in the spectra is difficult to visualize, as the Si $L_{2,3}$ edge for most silicates is barely visible against the monotonically decreasing background. This is primarily due to noise resulting from channel-to-channel gain variations of the photodiode detector [16].

Particles synthesized with an $Ar+N_2$ plasma (with the same reactant flow rates and deposition temperature as in the $Ar+H_2$ case) showed a very different morphology. The particles in this case were agglomerated. An EDS linescan of a representative structure shows the presence of Ti, Si and N, but with little oxygen (Fig. 8). The corresponding PEELS spectra confirm the presence of Ti, Si, and N, and again indicate a lack of oxygen (Fig. 9).

Samples collected for the two cases show significant differences. We observed discrete $TiSi_x$ and TiN_x particles with an $Ar+H_2$ plasma, while with an $Ar+N_2$ plasma we

Fig. 9. PEELS spectra of the nanostructure synthesized using an $Ar+N_2$ plasma.

found agglomerated structures. Samples prepared with N_2 as one of the plasma gases resembled the coatings in terms of composition, as they contained Si, Ti and N. On the other hand, the spherical or cube-like structures from the $Ar+H_2$ case contained only two of the three elements. The difference between the two systems can be partly attributed to the effect that increased N_2 flow has on the phase stability of the Si–Ti–N system by allowing the formation of a stable silicon nitride phase.

3.4. In-situ size distribution measurements

In-situ size distribution measurements were performed to characterize the impacting particles that form our coatings. Our measurements show that the mode of the size distribution lies in the range 10–15 nm (Fig. 10). It is worthwhile to note that changing the plasma gas mixture made only a small difference in particle size distributions. This emphasizes the fact that the morphological differences we observed in the TEM were due to changes resulting from an increased nitrogen partial pressure.
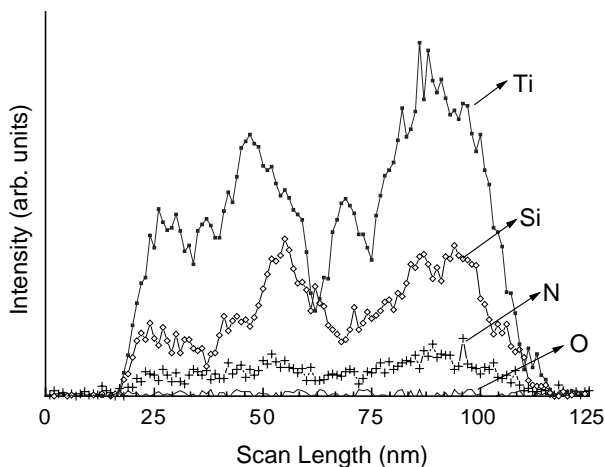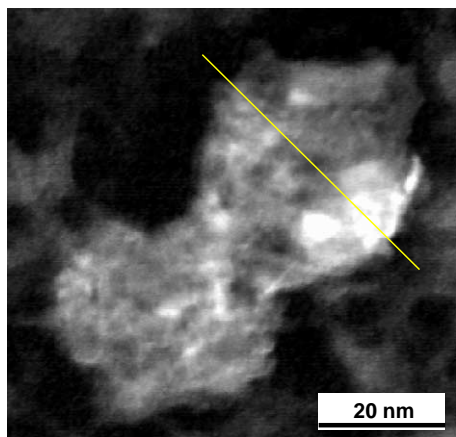

Fig. 8. EDS linescan of an agglomerated nanostructure synthesized using an $Ar+N_2$ plasma and collected on a TEM grid utilizing the aerodynamic lenses. The scan was taken along the line shown on the TEM image.
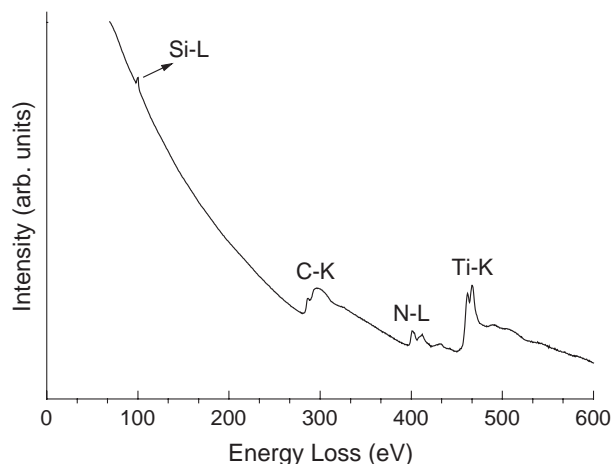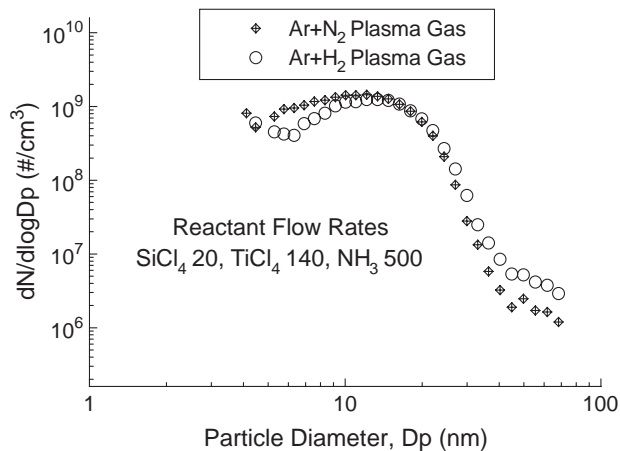

Fig. 10. In-situ size distribution measurements of Si–Ti–N for the different plasma gases with identical reactant flow rates (listed in sccm).

4. Conclusion

The effect of process parameters on the structure of Si–Ti–N coatings deposited by high velocity impaction of nanosized particles was investigated. When the plasma gases contained Ar+H_2, crystalline phases in the coatings consisted of TiN, $TiSi_2$, and Ti_5Si_3. When the system was switched to a plasma gas mixture of Ar+N_2, the only crystalline phase was TiN. Transmission electron microscopy of a film sample obtained through FIB milling confirmed the presence of TiN crystallites in an amorphous matrix. The fact that crystallite sizes are larger than 10 nm is thought to be a primary reason that HPPD-synthesized coatings have not been superhard, although they are harder than standard TiN. Analytical TEM analysis of particles deposited by aerodynamic lenses showed significant differences in morphology when the plasma gas composition was changed. The differences can be attributed partly to the effect of extra N_2 flow on the phase stability of the Si–Ti–N system. In-situ particle diagnostics showed only small changes in the particle size distributions when the plasma gases were changed.

Acknowledgements

References

[1] F.-J. Haug, L. Bonderer, P. Schwaller, J. Patscheider, M. Tobler, A. Karimi, Comput. Sci. Tech. 65 (2005) 799.
[2] N. Jiang, Y.G. Shen, Y.-W. Mai, T. Chan, S.C. Tung, Mater. Sci. Eng., B 106 (2004) 163.
[3] S. Vepřek, S. Reiprich, Thin Solid Films 268 (1995) 64.
[4] S. Vepřek, A. Niederhofer, K. Moto, T. Bolom, H.-D. Männling, P. Nesladek, G. Dollinger, A. Bergmaier, Surf. Coat. Technol. 133–134 (2000) 152.
[5] H. Watanabe, Y. Sato, C. Nie, A. Ando, S. Ohtani, N. Iwamoto, Surf. Coat. Technol. 169–170 (2003) 452.
[6] J. Hafiz, X. Wang, R. Mukherjee, W. Mook, C.R. Perrey, J. Deneen, J.V.R. Heberlein, P.H. McMurry, W.W. Gerberich, C.B. Carter, S.L. Girshick, Surf. Coat. Technol. 188–189 (2004) 364.
[7] P. Liu, P. Ziemann, D.B. Kittelson, P.H. McMurry, Aerosol Sci. Tech. 22 (3) (1995) 293.
[8] F. Di Fonzo, A. Gidwani, M.H. Fan, D. Neumann, D.I. Iordanoglou, J.V.R. Heberlein, P.H. McMurry, S.L. Girshick, N. Tymiak, W.W. Gerberich, N.P. Rao, Appl. Phys. Lett. 77 (2000) 910.
[9] X. Wang, J. Hafiz, R. Mukherjee, S.L. Girshick, J.V.R. Heberlein, P.H. McMurry, Plasma Chem. Plasma Process 25 (2005) 439.
[10] S.L. Girshick, J.V.R. Heberlein, P.H. McMurry, W.W. Gerberich, D.I. Iordanoglou, N.P. Rao, A. Gidwani, N. Tymiak, F. di Fonzo, M.H. Fan, D. Neumann, in: K.L. Choy (Ed.), Innovative Processing of Films and Nanocrystalline Powders, Imperial College Press, London, 2002.
[11] L.A. Giannuzzi, F.A. Stevie, Micron 30 (1999) 197.
[12] S. Sambasivan, W.T. Petuskey, J. Mater. Res. 9 (1994) 2362.
[13] B.E. Warren, B.L. Averbach, J. Appl. Phys. 23 (1952) 497.
[14] S. Vepřek, Vac. Sci. Technol., A 17 (1999) 2401.
[15] S.P. Murarka, Silicides for VLSI Applications, Academic Press, Florida, 1983, p. 144.
[16] A.J.L. Garvie, P.R. Buseck, Am. Mineral. 84 (1999) 946.